Available online at www.sciencedirect.com

ScienceDirect

Procedia Manufacturing 00 (2019) 000–000

Procedia MANUFACTURING

www.elsevier.com/locate/procedia

30th International Conference on Flexible Automation and Intelligent Manufacturing (FAIM2021)
15-18 June 2021, Athens, Greece.

Inline Quality Control for Thermoplastic Automated Fibre Placement

A. Schuster[a,*], M. Mayer[a], M. Willmeroth[a], L. Brandt[a], M. Kupke[a]

[a]*German Aerospace Center (DLR), Center for Lightweight Production Technology, Am Technologiezentrum 4, 86159 Augsburg, Germany*

Abstract

Aerospace production is relying heavily on quality assurance, especially for lightweight materials such as carbon fiber reinforced plastics (CFRPs). Due to the sequential organization of manufacturing and quality assurance lead times for parts and machine downtime are increased. An example is the highly automated process of thermoset tape laying, where every ply is manually inspected. Customized solutions to integrate quality assurance do exist, however mainly for specific processes and hardware. This leads to costly, isolated and non-transferable systems. At the Center of Lightweight Production Technology in Augsburg, Germany a more versatile and modular concept for inline data acquisition, storage and evaluation is investigated. On the basis of a laser line and camera system a generic inline measurement system for automated fiber placement (AFP) is developed, that is capable to inspect a variety of quality aspects such as positional tolerances and material properties. In a database driven approach the collected data is stored and analyzed. This paper presents the generic inline measurement system, the data storage system and the obtained measurement results for a thermoplastic AFP process. Additionally suggestions for future improvements and possible applications are described.

Keywords: Inline quality control; automated production; real time data acquisition; automated fibre placement

1. Introduction

2. Thermoplastic Automated Fibre Placement

Thermoplastic Automated Fibre Placement (T-AFP) is a relatively new process route for high performance aerospace part generation. Thermoplastic structural parts for aerospace applications promise a big advantage over their thermoset counterparts: the ability of being joined by welding may simplify the final assembly. Pre-equipped functional units could be joined without drilling and thus contaminating the sensitive system installations by the else unevitable carbon-matrix dust. Up to now except of technology demonstrators only comparably small thermoplastic high performance parts exist, because consolidation is a crucial step. Press consolidation gives best results, is complex, tools are costly and part size is limited. Vacuum bag consolidation often suffers from insufficient consolidation pressures and auxiliary materials like tacky tape or vacuum bags degenerate under oxygen atmosphere at higher process temperatures. Autoclave consolidation again is costly and suffers also from auxiliary material degradation albeit less critical because of the inert atmosphere.

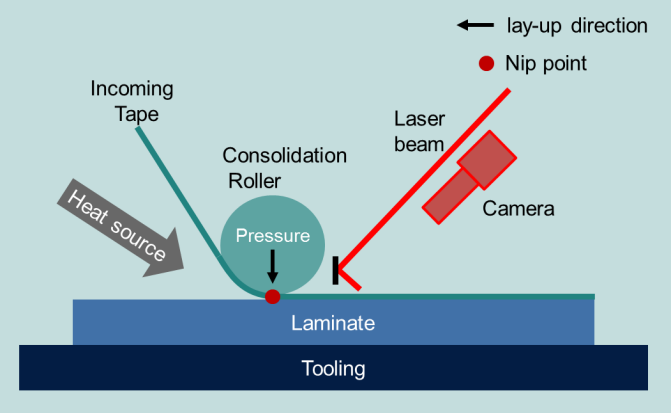

Figure 1. Principle of T-AFP process with inspection system attached

* Corresponding author. Tel.: +0-000-000-0000 ; fax: +0-000-000-0000.
E-mail address: Alfons.Schuster@dlr.de (M. Kupke).

2.1. Material and Process

Based upon the well developed Automated Fibre Placement (AFP) tape laying technology T-AFP offers another opportunity: In contrast to AFP thermoplast (PPS, PEEK) impregnated semi-finished goods are used for the preform process instead of conventional prepreg tows (carbon fibres impregnated with reactive resin). Since the material is melted and brought into intimate contact with the layers below, a so called in-situ consolidation may be achieved allowing a processing without a press, an oven or an autoclave (Fig. 1).

One limitation may lie in the high-power lasers which serve as heat source to reach the tape's melting temperature of ≈400 °C that require factory-wide laser safety zones. Xenon-Flashlamps can be used as an alternative heat source and give hope for less requirements concerning eye-safety and thus overcoming the limitations introduced by a laser [1]. After all, the T-AFP process offers many chances and may prove as key technology for future aerospace part production.

2.2. Defects in Automated Layup

Since the laminate is made up of hundreds of meters of tape, quality control is essential and should be performed automatically and during layup. An excellent and brief overview of every possible defect type in AFP is given in [2]. Breaking down the possible defect types into categories the author distinguishes between imprecise positioning, improper bonding, foreign anomalies and tow anomalies. All defect categories can be captured by 3D imaging (typical for AFP is laser light sheet measurement [3] or optical coherence tomography [4]) and evaluating the three dimensional height profile of the scanned region. Gaps, overlaps and missing tows can be detected inline by evaluation of single profiles while all other defect's recognition is somehow "offline", since a plurality of profiles has to be considered before a defect can be properly identified. Thus, evaluation can be split up in a fast, inline part yielding results immediately but being limited to gaps, overlaps and tow position, and a more or less delayed part yielding results as soon as the entire defect has been scanned. For the proper classification of defects like early or late tape adds or cuts or missing tows more information about the desired tow position is required making the evaluation even less inline and dependent on the availability of those meta information.

3. Inspection Hardware

3.1. Camera and Illumination

For our research we chose a laser light sheet measurement setup (see Fig. 2 for the measurement principle) originally designed by Infactory Solutions [3], comprising a cased 3B-Class 660 nm line laser with 90° deflection mirror and a 45° tilted camera with also cased optics, giving a ±45° inspection geometry suitable for the highly reflective carbon fibers (figure 3). Laser and camera are commercially available, well supported

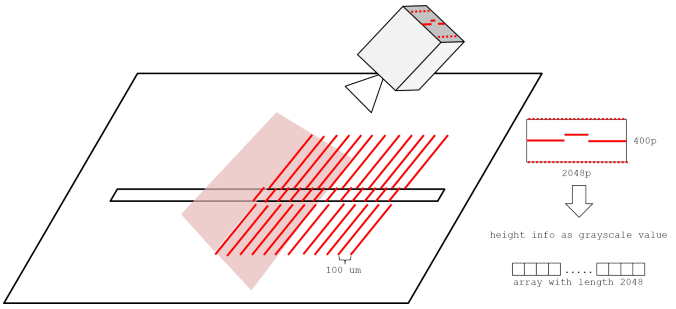

Figure 2. Operating principle of laser light sheet triangulation: the incident laser line is displaced depending on the specimen height. The camera grabs images and computes a height profile on the basis of the displacement.

standard products, which is a plus for later industrial applications. Camera resolution is 2048 x 2048 Pixels yielding a measured resolution of 39.4μm in the focal plane. The camera's internal light sheet measurement algorithm uses 4 bit subpixel approximation for determining the laser line position which leads to a theoretical depth resolution of 39.4 $\mu m/(16\sqrt{2}) = 1.74\ \mu m$ in good accordance with the measured value of 1,77 μm that was derived from a 5 mm step. The depth resolution proved to be non-gaussian distributed, meaning that obtaining a result that matches the pixel resolution is six times more probable, yielding only 71 % of subpixel values instead of the expected 94 %, what we chalked up to algorithm internals. Nevertheless the material thickness of 0.2 mm height proved to be well measureable as desired. The camera is equipped with a band pass filter matching the laser wavelength in order to exclude ambient light. Since the heating of the tows is done by a high power flash lamp the band pass filter is not sufficient to exclude all flash light immissions, so a housing as a beam shield may be indicated later on.

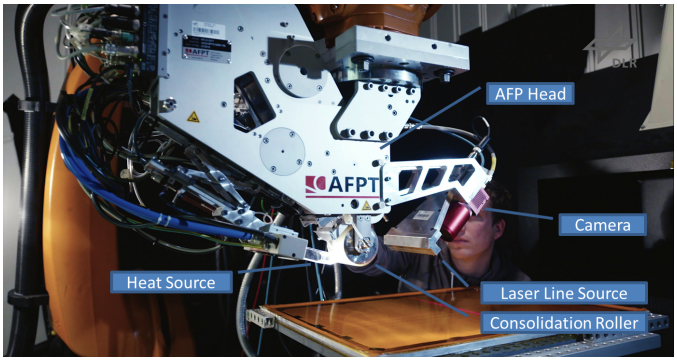

Figure 3. Robot cell setup with AFP-head, heat source, laser line source and camera

3.2. Profile Generation and Triggering

The camera is equipped with a RS422 standard encoder interface, allowing hardware triggering of profile acquisition. Whenever a trigger is received, the camera grabs an image and calculates the height profile by analyzing the pixel displacement. The profile is stored in camera memory together with encoder count and time stamp, allowing a later determination of

the real world position where the profile was acquired. Whenever a predefined number of profiles has been acquired, the profile chunk is transferred to a ring buffer and can be read out. The profile chunks are stored in memory and stitched to a single image after the acquisition of the actual track is finished. At this moment, the robot will stop and reposition to start the next track and the measurement system has time to store the data to the harddrive and to start uploading the track data to the database.

4. Acquisition Software

Since our use case is thermoplastic T-AFP, not thermoset AFP, algorithms for defect recognition suitable for AFP proved to be not applicable here. Especially the production standards defining which anomalies are to be regarded as defects are not yet elaborated for T-AFP and are the subject of ongoing investigations. This means that it is advantageous to store all measurement data together with process data from the robot and the AFP-head plus additional meta-data in a database to allow a broad base evaluation in order to refine the production standards for T-AFP.

The software bundled with the inline measurement system by Infactory Solutions does not allow flexible use on different environments and direct data access during acquisition, as well it is limited to a proprietary database disallowing the integration to DLR's integrated data management system (IDMS) that allows correlation with a plenty of additional data. Starting from scratch a generic acquisition software overcoming those limitations was developed. As image acquisition is very hardware-related and speed is an issue C++ was chosen as a basis together with Stemmer Imaging's Common Vision Blox GigE-Vision acquisition library.

4.1. Profile Acquisition

As mentioned in section 3.2 the profile chunks are available as soon as a certain number of profiles has been acquired. Acquisition is running in a separate thread waiting for available profiles. As soon as a profile chunk comes in, the profile data are separated from the chunk info and both is stored in memory.

4.2. Positional Synchronization

In essence, the profiles must be triggered by the robot movement. This can be done by equipping the consolidation roller with an encoder or, in our case, using the robot's built in path synchronous triggering. We used KUKA's technology package "Fast send driver", which allows path synchronous triggering and sends a UDP-Packet with the actual robot position whenever the trigger signal is activated. Naturally, another thread is appropriate in order to watch out for incoming positional data and storing them in memory.

4.3. Data Storage

Before storing the data the fusion of the two asynchronous data sources for profiles and trigger positions has to be done. Both acquisition threads are stopped and the robot position for every profile is associated with the profile. Now, the data is checked in to our integrated data management system (IDMS) (Fig. 4) by another asynchronous thread allowing immediate resumption of the measurement. In fact, there is a thread pool to avoid data loss in the case of temporally overlapping check ins.

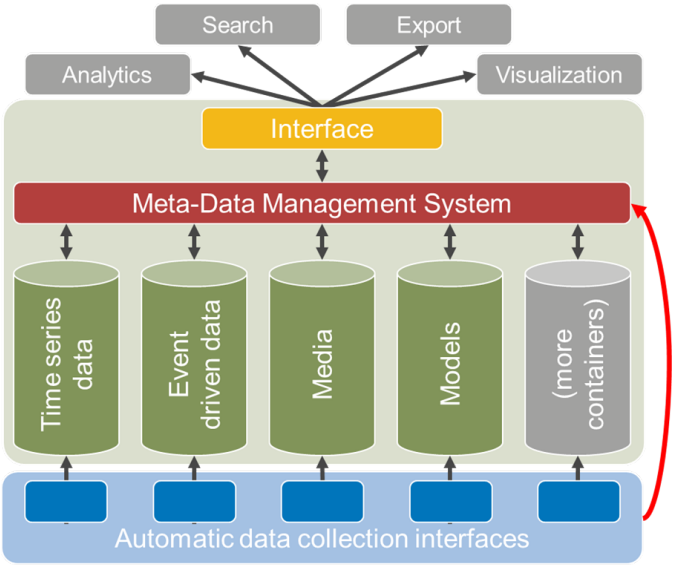

Figure 4. Integrated data management system as prototyped by DLR

The IDMS not only holds data from the measurement system: Environmental data, material data, robot readings, sensor and status readings from the T-AFP head and other devices are stored in specific containers with a superseding graph oriented database that allows correlation of a vast variety of data in order to find out process key parameters and to ensure traceability of data over a plenty of production runs. Further data for quality control like thermography or ultrasound inline measurements are also made available and can present a holistic picture of what really happened to the part during production [5].

5. Geometric Transformations

5.1. Calibration

One point of importance is that all profile data up to now are in arbitrary pixel units. To convert this to real 3D profiles several steps are necessary. After detrending the lateral (x) pixel coordinates are converted to real world distances from the profile center. To do so we took the profiles of a steel tape measure from different distances. The etched scale marks are well defined in the profiles so this is a fast and cheap way of calibrating. In the desired measurement range of ±3 mm we found only neglectable variations in scale.

Having done this every pixel has to be shifted by it's z-value in the measurement (y) direction, since our inspection geometry is ±45° and different heights of the measured object are hit by th laser beam at different y-positions.

5.2. Point Cloud Generation

To convert the profile into real world coordinates, a set of transformations is needed. Going from the robot's TCP the beam position with respect to the TCP is concatenated resulting in a coordinate system, where the profile is lying in the xz-plane. The calibrated profile values can now be transformed into robot base coordinates which may be converted back to CAD coordinates in order to form a digital twin (Fig. 5).

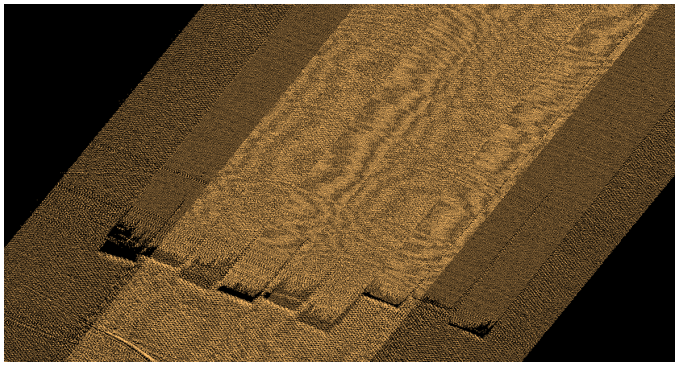

Figure 5. Generated pointcloud for a testing plate layup. Three scans are superimposed resulting in a higher point density in the overlapping pars in the middle of the pointcloud.

6. Data Evaluation

6.1. Outlier Removal and smoothing

Both noise and erroneous data are crucial for a proper evaluation. Noise in some cases can't be avoided, since it may be caused by material properties. In our case it was not possible to perform a noise free profile acquisition, because the laser reflection strongly depends on the incident angle and the tape surface is not smooth enough to keep the imaged laser line as perfect as one would desire for measurement purposes. Another aspect was the noisy (rough) background, that is causing evaluation problems. Therefore, we decided to blur the profile image with a 8 by 25 pixel kernel. We found this to be not satisfactory, because blurring the outliers resulting from beam shading (the beam "slips" under the tape when the tape start is not properly bonded) or stray light (exclusively from the heating flash lamp) doesn't make the outliers vanish but smears their intensity distribution in an uncontrollable manner. The solution was smoothing with a mask [6], where the influence of masked pixels can be almost excluded by smoothing both image and mask and subsequently dividing the smoothed image pixelwise by the smoothed mask.

In order to detect the outliers defining which image parts should be masked we found that profiles with outliers (influenced by the flashlamp) can be distinguished from normal scans by calculating the Minkowski–Bouligand or boxcount dimension [7] as shown in figure 6.

The corresponding formula is

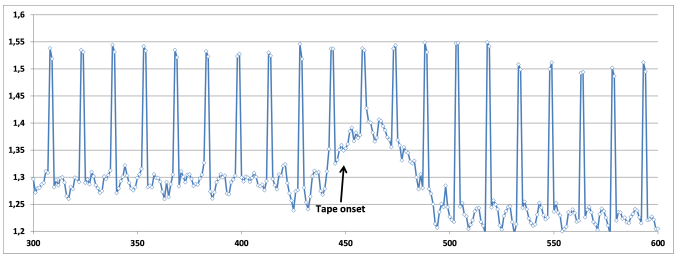

Figure 6. Minkowski–Bouligand dimension for 1000 profile scans on background (left) ant tape (right). Outliers caused by flash lamp stray light can be easily identified by a dimensional value ≥ 1.4.

$$D = \lim_{\epsilon \to 0} \frac{\log N(\epsilon)}{\log \frac{1}{\epsilon}}$$

what means in practice that the boxcount dimension of a straight line is 1 and is approaching 2 for a signal bouncing from maximum to minimum for every reading.

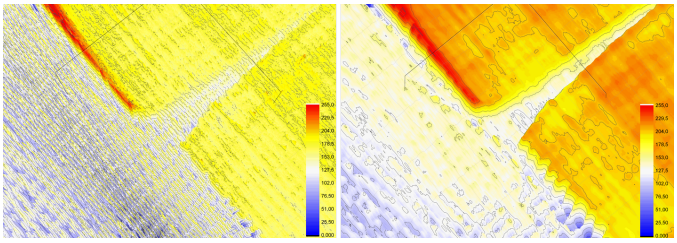

Figure 7. Acquired profiles with and without smoothing and outlier removal (pixel coordinates and arbitrary height units)

Figures 7 and 8 show the results of the procedure. Outliers are successfully eliminated and the smoothed profiles now reveal the information relevant for evaluation (see horizontal profiles in Fig. 8).

6.2. 2.5D-Evaluation

Previous research showed that pointcloud evaluation is very hard to perform. So we decided to explore a simplified evaluation procedure taking the profiles as a depthmap where the pixel coordinates correspond to x and y direction and the pixel value corresponds to the z-value or profile height. This neglects the exact calibration from 5.1 but is a good enough approximation for evaluation with standard computer vision or machine learning algorithms that are most suitable for image analysis. Having done this the defects may be mapped to the 3D pointcloud after evaluation.

There is research on the machine learning sector to overcome the ubiquitous lack of training data by simulation [8], but for the moment we stick on to computer vision where less data is required and postpone machine learning approaches until we have more data in the database. Further, computer vision can be a good assistance for properly annotating the training data in

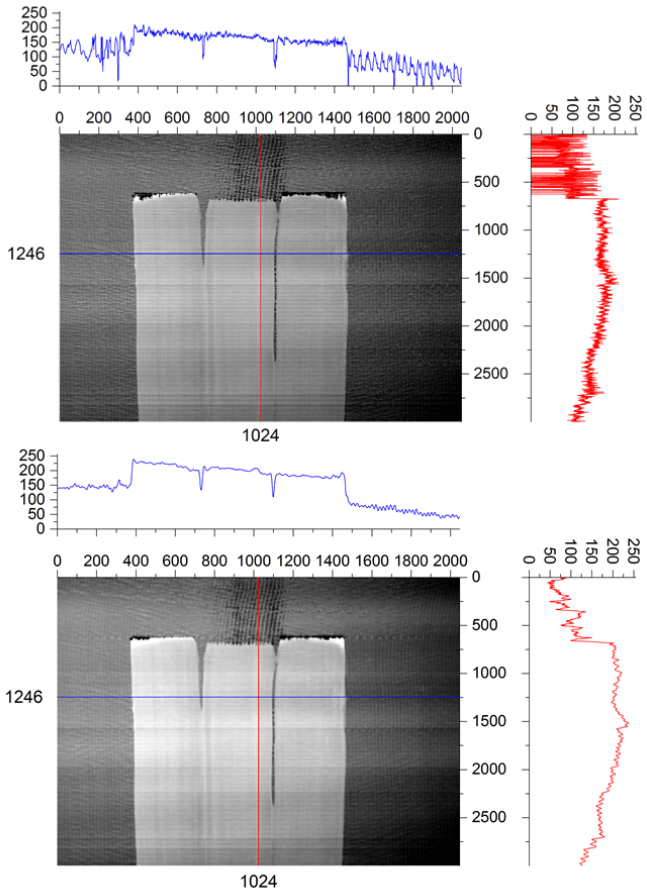

Figure 8. Acquired profiles with and without smoothing and outlier removal (pixel coordinates and arbitrary height units)

a fast manor, what is another ubiquitous drawback of machine learning.

7. Inline Capability

As mentioned in section 2.2 there are defects that allow inline evaluation, namely gaps, overlaps and missing tows. All this boils down to 2D profile evaluation. Having smoothed the

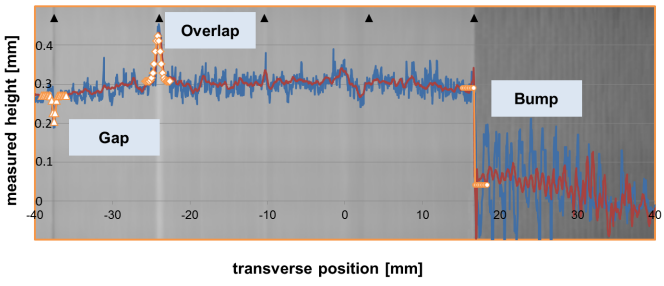

Figure 9. Example of profile evaluation. The triangles show the nominal tape end positions, blue is original profile, red is smoothed.

profiles as described in 6.1 the profiles can be evaluated. Since the tape ends are known and vary only slightly it is possible to consider only a narrow region of interest (ROI) around the assumed tape ends. We found a zone of ±2.5 mm corresponding to 128 Pixels to be sufficient and even stabilizing for the algorithm. Curve-Fitting can then be used to determine gaps, overlaps and bumps. First promising results were obtained by fitting the data with a Gaussian function for gaps and overlaps and a Heaviside step function for steps at the tape ends (Figure 9). For increasing performance and stability the non linear Gaussian fit was replaced by an approximation with a parabola, which is linear concerning the fit parameters and always yields a well-defined solution (for details compare section 7.1.3). If neither gap nor overlap is detected (insufficient height or vertex out of position or too weakly curved), the Heaviside function is simplified by analyzing minimum and maximum of the derivative of the median-filtered height profile.

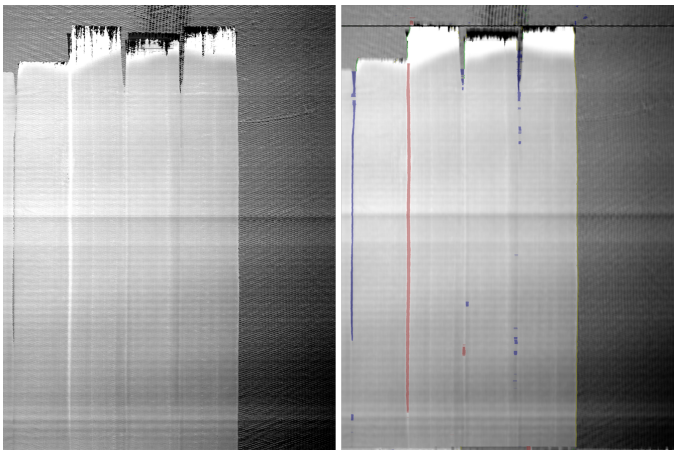

Figure 10. Results of inline evaluation of gaps, overlaps and tow border

A sample for the evaluation is given in Figure 10, where one gap (in the last track), one overlap (at the left track edge) and the right tow border were detected (colored parts in right image). The evaluation seems pretty stable as long as the material is smooth and may be improved further by median filtering the detections in order to eliminate erroneous outlier detections for “noisy” materials. Another point to improve is the transition from very wide gaps and overlaps to a set of two bumps.

7.1. Speed Issues

The desired layup speed is in the range of 0.1 m/s with the option for later increase. Assuming a resolution of 0.1 mm in the layup direction the profile acquisition rate is 1 kHz , what has to be considered in triggering, acquisition and evaluation.

7.1.1. Trigger Speed

For the moment the trigger speed of the robot is limited to 1kHz what is sufficient for the moment but may cause issues in the future. On the robot side there is no potential for increase, so we are evaluating both hardware pulse multiplication with PLL (phase locked loop) or microcontrollers. Otherwise, we would need to go back to an encoder mounted to the consolidation roller what has other drawbacks (accessibility, rolling length of rubber coated roller ≠ geometric length).

7.1.2. Acquisition Speed

The Automation Technology C5-2040-4M camera can be a very fast profiling camera. Profile speeds up to 25 kHz are possible, but only if the area of interest (AOI) window is 8 Pixels high. On the other hand the profiling speed drops down to 180 Hz when imaging with 2048 pixel AOI height. With a AOI of 360 pixels height an acquisition rate of 1 kHz can be accomplished with a not too strong limitation in detectable height difference of ≈ ±10 mm, which could be extended by AOI-tracking later on. Aiming at higher speeds AOI-tracking will certainly be required.

7.1.3. Evaluation Speed

As mentioned above the profile ROI is 128 pixels with in our case four ROIs for three tapes, making a total of 512 pixels to be evaluated. We used a simplified model where we fitted a polynomial of second degree (parabola) through the upper half of the points around the maximum (Fig. 11). Despite

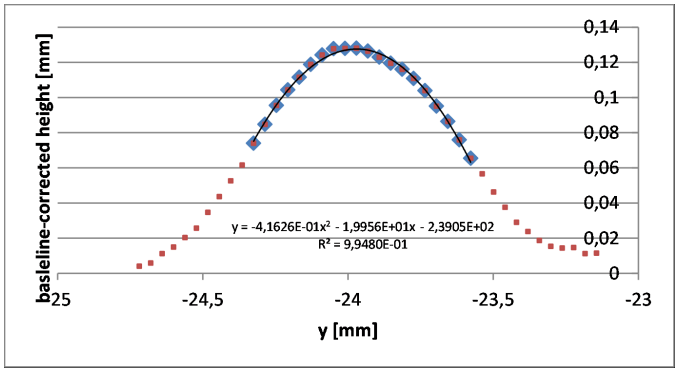

Figure 11. Example of profile fit (overlap in Figure 9)

of the simplicity of th model, the fit is in good accordance with the data. Polynomial fits are linear and thus always have a well defined solution and a good performance. On our test system (quad core Intel Core I7-4930MX @ 3GHz) we measured an overall detection time of 140 µs for all four tape borders with single core and 35 µs with quad core evaluation using the Open Multi-Processing API (OpenMP). Multicore processing with OpenMP proved not to give any speed gain for single profiles most likely due to the already short processing time. Speed gains as described above could only be obtained for the calculation of several hundreds of profiles. In general multicore processing should only be applied to chunks of profiles, which is the natural way the camera delivers data. So inline evaluation is feasible for the actual speeds and may be implemented for higher speeds in chunk evaluation mode with a small temporal delay.

7.2. Geometric Limitations

7.2.1. Trailing Measurement

One major drawback for the use of a laser light sheet system in combination with the highly reflective carbon tapes is it's big geometric footprint. In the current setup the laser line is located ≈95 mm behind the nip point and this distance can"t be further reduced due to the consolidation roller and reflection mirror geometry. This means that every layup track has to be prolonged by ≈100 mm staying on the laminate resulting in unwanted overhead in program generation.

7.2.2. Distance Variation

Another limitation is the camera's low focal depth. In order to get enough light to the camera chip the iris has to be wide open, resulting in a low tolerance against distance variation. This also leads to programming overhead as well as to limitations on highly curved geometries, because the boundaries introduced by the consolidation roller and the cameras focal depth can't be satisfied simultaneously. This is not an issue for our facilities during the next years because the manufactured parts will be considerably large, but may be a future challenge.

8. Summary and Outlook

Starting from scratch with profile acquisition on a laser light sheet measurement system we made good progress in data acquisition and evaluation. Gaps and overlaps can be detected inline and there is still speed reserve. Measurement on our T-AFP robot is running flawless and we are looking ahead to the next parts in order to gain more data and to detect further defect classes. With DLR's integrated data management system the path to automated defect recognition of every possible defect in the future is clear. Final challenge will be refining the production standards for thermoplastic automated fibre placement together with industrial partners.

9. Acknowledgements

Special thanks go to the thermoplastic composites team of ZLP Augsburg that made this research possible by giving us the chance to monitor the quality inline.

References

[1] L. Brandt, D.Deden, F. Fischer, P. Dreher, N. Patrik, D. Williams, M. Engelschall, D. Nieberl, S. Nowotny, Xenon flashlamp based in-situ automated fiber placement of thermoplastic composites, ICCM22 (2019), Melbourne, Australia

[2] K. Schlegel, P. Parlevliet, C. Weimer. A. Schuster, M. Kupke, A literature review of quality control for automated lay-up processes of CFRP, Journal of Plastics Technology 15 (2019), 392-436

[3] G. Gardener, Infactory Solutions qualifies AFP sensor on MTorres equipment with Airbus, Composites World (2017), https://www.compositesworld.com/blog/post/infactory-solutions-qualifies-afp-sensor-on-mtorres-equipment (accessed 19. 2. 2020)

[4] In-process Inspection for AFP (2020), https://www.jec-world.events/de/essential_grid/in-process-inspection-for-afp (accessed 10. 2. 2020)

[5] L. Brandt, Inline Quality Assurance for tape laying processes, Ariane Group 10th R&T Days (2019) on Materials and Structures: High Performance at Competitive Cost, CETIM, Senlis

[6] Smoothing with a mask, https://answers.opencv.org/question/3031/smoothing-with-a-mask/ (accessed 19. 2. 2020)

[7] Minkowski–Bouligand dimension, https://en.wikipedia.org/wiki/Minkowski-Bouligand_dimension (accessed 19. 2. 2020)
[8] S. Zambal, C. Heindl, C. Eitzinger, Machine Learning for CFRP Quality Control, Zenodo (2019), http://doi.org/10.5281/zenodo.3381930 (accessed 19. 2. 2020)